Detection Performances of Evil Waveform Monitors for the GPS L5 Signal

Paul Thevenon, Quentin Tessier, Denis Maillard, Margaux Cabantous, Francisco Amarillo-Fernández, Filipe de Oliveira Salgueiro, Olivier Julien

HAL Id: hal-01094176

https://enac.hal.science/hal-01094176

Submitted on 11 Dec 2014

Detection Performances of Evil Waveform Monitors for the GPS L5 Signal

P. Thevenon, O. Julien, Q. Tessier, *ENAC*. D. Maillard, M. Cabantous, *Capgemini*.
F. Amarillo-Fernández, F. De Oliveira Salgueiro, *ESA*.

BIOGRAPHIES

Dr. Paul Thevenon graduated as electronic engineer from Ecole Centrale de Lille in 2004 and obtained in 2007 a research master at ISAE in space telecommunications. In 2010, he obtained a PhD degree in the signal processing laboratory of ENAC in Toulouse, France. From 2010 to 2013, he was employed by CNES, the French space agency, to supervise GNSS research activities and measurement campaigns. Since the July 2013, he is employed by ENAC as Assistant Professor. His current activities are GNSS signal processing, GNSS integrity monitoring and hybridization of GNSS with other sensors.

Dr. Olivier Julien is the head of the Signal Processing and Navigation (SIGNAV) research group of the TELECOM laboratory of ENAC, in Toulouse, France. He received his engineer degree in 2001 in digital communications from ENAC and his PhD in 2005 from the Department of Geomatics Engineering of the University of Calgary, Canada. His research interests are turned towards the use of satellite-based navigation systems for safe navigation.

Quentin Tessier graduated as an electronics engineer from ENAC in 2013. He has worked at ENAC for one year as a research assistant on GNSS signal processing for signal quality monitoring and multipath mitigation. He is now a PhD student at ENAC working on SBAS autoland models.

Margaux Cabantous graduated as an electronic and telecommunication engineer from the Ecole Nationale de l'Aviation Civile in 2014. She performed its engineer internship in Capgemini Bayonne working on the adaptation of RIMS-C EWF algorithm on L5 pilot signal. She currently works as a GNSS engineer in Capgemini on signal processing subjects.

Denis Maillard received his engineer degree in Electronic and Computer Engineering from Institut National des Sciences Appliquées de Rennes in 2010. Since 2011 he works as a GNSS engineer in the EGNOS team of Capgemini Bayonne. He is currently in charge of the activities linked to GNSS signal processing.

Francisco Amarillo-Fernández received his Master's Degree in Telecommunication by the Polytechnic University of Madrid (UPM) Spain in 1997, and his Master's Degree in Surveying Engineering by the UPM in 1992. He has been working for the ESA Navigation Directorate since 2001 and has participated/led in numerous research activities in the GNSS field since 1997.

Filipe De Oliveira Salgueiro studied at the Instituto Superior Técnico in Lisbon, Portugal, where he accomplished the Master of Science in Aerospace Engineering in 2014. He has been working since 2012 at the European Space Agency in ESTEC on the Radio Navigation Systems and Techniques Section. Subject of work includes: GNSS integrity, SVS, evil waveforms and other GNSS activities.

ABSTRACT

Evil Waveform (EWF) are signal distortions that can create persistent errors (bias) on the pseudo-range measurement of several meters. They are of particular interest for differential GPS users and for safety critical users. For instance, differential corrections do not remove this bias if the reference receiver and the rover receiver use different receiver parameters (notably RF input bandwidth and correlator spacing).

In order to protect Civil Aviation users from this kind of errors, the ICAO has standardized a model for this failure, which can then be monitored by high-integrity systems such as SBAS and GBAS. In parallel to the standardization of the model, a family of Signal Quality Monitoring (SQM) techniques has been established for GPS L1 signal.

With the appearance of the new GPS L5 signal, Civil Aviation users will be allowed to benefit from increased positioning performances. However, it is necessary to extend the signal deformation models and detection metrics to this new signal.

This study uses data collected from modern receivers to evaluate the performances of SQM techniques on L1 C/A and L5 pilot signals. The methodology for establishing the detection thresholds is detailed and applied to 4 different datasets. The results show that the legacy SQM techniques does not reach the required performances when using modern receivers, which have larger pre-correlation bandwidth. For L5 users, an adaptation of the SQM techniques provides compliant results.

The study also discusses the performances experienced by different types of users (from unmonitored independent users to differentially-corrected, protected users) and the dependency of the monitoring performances with regard to the receiver parameters.

Finally, the paper also discusses the use of a statistical description of collected measurements, which may not provide enough information to correctly model the metrics distribution.

INTRODUCTION

Evil Waveforms are signal distortions that are attributed to a payload anomaly. They can create persistent errors (bias) on the pseudo-range measurement of several meters, without the receiver loosing lock. They are a particularly dangerous threat for differential GPS users, because differential corrections do not remove this bias if the reference receiver and the rover receiver use different receiver parameters (notably RF pre-correlation bandwidth and correlator spacing).

The first occurrence of Evil Waveform occurred in 1993 on SVN19, with a differentially corrected vertical error up to 8 m when SVN19 was taken into account for the position computation, compared to a position when it was excluded [1]. The origin of the error was shown to be at the signal generation unit, onboard the satellite payload.

In order to protect Civil Aviation users from this kind of errors, the ICAO has standardized a model for this failure [2], which can then be monitored by high-integrity systems such as SBAS and GBAS.

A family of monitoring techniques has been developed and implemented in these systems in order to comply with the ICAO requirements. These techniques, named Signal Quality Monitoring (SQM), are based on the observation of the correlation function of the received signal to check if unexpected deformations are present. A founding work for this category of monitoring technique is described in [3].

However, the ICAO model is only defined for the GPS L1 C/A and GLONASS L1 signals, and SQM has only been standardized for GPS L1 C/A signals. With the introduction of a new signal for Civil Aviation users, it is relevant to study if the existing SQM techniques are efficient to monitor GPS L5 pilot signal. Also, modern receivers have different characteristics for processing GPS L1 C/A signals than receivers used during the initial definition of SQM techniques, notably a larger pre-correlation bandwidth. This difference may impact the SQM performances.

The aim of this paper is to assess the performances of SQM technique on L5 and modernized GPS L1 C/A receivers.

The paper has the following structure. First, the ICAO EWF Threat Model will be adapted to the GPS L5 signal. Secondly, the existing Signal Quality Monitors will be adapted to the GPS L5 signal case. The process to determine the detection threshold will be described and applied to GPS L5 and GPS L1 C/A signals collected with modern receivers. In a third part, the SQM performances will be studied for different types of users. In a fourth part, the SQM performances will be studied in different region of the User Design Space, corresponding to different receiver parameters. A fifth part will come back on some relevant lessons learned in this study through the use of a limited description of collected data based on correlator output statistics rather than complete time series.

THREAT MODEL ADAPTATION TO GPS L5 SIGNALS

Existing ICAO TM for GPS L1 C/A signals

ICAO [2] identifies 3 types of effects on the correlation function of GNSS signals created by an Evil Waveform that can lead to misleading information:
- Dead zones, ie zones where the correlation function is flattened,
- False peaks, ie multiple zones toward which the tracking process can lock,
- Distortions, ie deformation around the correlation peak, which creates a bias on the range estimate.

The ICAO threat model has 3 parts, noted as TM-A, TM-B and TM-C, that can create the 3 correlation peak pathologies listed above.

Threat Model A consists of the normal C/A code signal except that all the positive chips have a falling edge that leads or lags relative to the correct end-time for that chip. TM A is defined by a single parameter Δ, corresponding to the lead ($\Delta < 0$) or lag ($\Delta > 0$) expressed in fractions of a chip. TM-A results in an offset of the correlation function and a flattening of the correlation peak.

Threat Model B consists of a second order filter applied to the normal C/A code signal. Threat Model B can be modeled by a second order linear system dominated by a pair of complex conjugate poles, located at $\sigma \pm j2\pi f_d$, where σ is the damping factor in nepers/second and f_d is the resonant frequency in Hz. The unit step response of the second order system is given by

$$e(t) = \begin{cases} 0 & \text{for } t \leq 0 \\ 1 - e^{-\sigma t}\left[\cos(2\pi f_d t) + \dfrac{\sigma}{2\pi f_d}\sin(2\pi f_d t)\right] & \text{for } t \geq 0 \end{cases}$$

Threat Model B results in oscillations around the slope changes of the autocorrelation function, in an asymmetric way.

Threat Model C is a combination of both previously described Threat Models

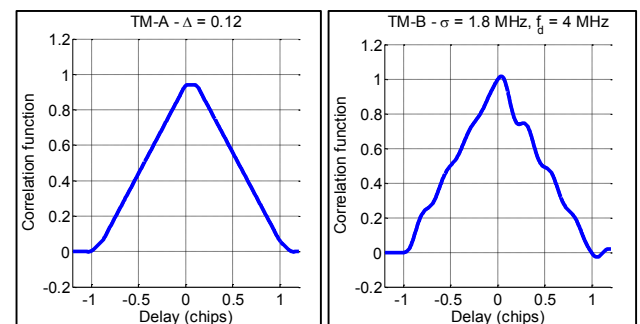The range of parameter values for each TM is given in Table 1.

Figure 1 – Correlation functions distorted by EWF

Adaptation of ICAO TM for GPS L5 signals

The GPS L5 signal is a new signal aiming at providing civil aviation users with a second signal, in addition to GPS L1 C/A. This second signal will provide to be more robust to interferences, and will permit to use dual frequency techniques to have an increased redundancy and also eliminate the first order term of the ionospheric delay, thus decreasing the budget error of the estimated pseudo-ranges and consequently increasing the accuracy of the position.
The GPS L5 signal is broadcast by the Block IIF satellites (first launch in 2010, 6 operational satellites in mid-2014), with an early demonstration in 2009 on a Block IIRM satellite (SVN 49). The signal is fully described in the public Interface Control Document [4].

The main differences of the GPS L5 and the GPS L1 C/A signals are:
1. An increased code rate: **10.23 MHz** for GPS L5 compared 1.023 MHz for GPS L1 C/A.
2. A different carrier frequency: **1176.45 MHz** for L5 compared to 1575.42 MHz for GPS L1.
3. The presence of **pilot and data components** transmitted in quadrature.
4. The L5 signal is defined in a bandwidth of **24 MHz** around the carrier frequency, while the L1/CA signal is defined in a band of 20.46 MHz around the carrier frequency.

In this analysis, we assume that the adapted threat model will not be impacted by the different carrier frequency and by the presence of a signal in the quadrature channel. More particularly, it is assumed that the pseudo-range measurements are provided by the pilot channel, and that only the pilot channel requires an EWF threat model.

It can be assumed that the signal generation unit onboard GPS satellites has a similar architecture for GPS L1 C/A and GPS L5 signals. Indeed, the modulation of the signal is the same except for the code rate. This assumption is confirmed in [5]. When observing the nominal deformations of the signal, they are very similar on L1 and L5 signals. We can therefore suppose from these observations that the same type and generation of components are used for the signal generation, and deduce that the failure mode, and hence the threat model, can be similar. **Therefore, the 3 types of Threat Models (A,B,C) are kept for GPS L5.** Only the ranges of parameters are to be adapted.

Table 1 –Threat Model parameters for GPS L1 C/A [2]

	Δ (chip)	σ (MNepers/s)	f_d (MHz)
TM A	[-0.12 ; 0.12]	-	-
TM B	-	[0.8 ; 8.8]	[4 ; 17]
TM C	[-0.12 ; 0.12]	[0.8 ; 8.8]	[7.3 ; 13]

To update the range of parameters for the L5 threat models, it is useful to look at the justification of the L1 C/A threat models given in [3].
The range for Δ is justified by the fact that lead or lags larger than 12% of the chip lengths would be easily detectable by multi-correlator techniques. Assuming that the same order of magnitude affects the L5 signal generation failure, this would relate to a chip length of 120% on L5. In order to be realistic with the tracking of GNSS signal, the lead or lag of a TM-A should be restricted to a value below the chip length. In addition, due to expected monitoring performance, a factor 1/2 has been applied to value for the L1 C/A model: it is expected that EWF with Δ over 60% of L5 chip will be easily detectable.
For the parameter f_d, the lower value for its range on L1 (4 MHz) is justified by the presence of specific monitors that would protect the military signal L1 P(Y). Since no such "military monitoring" is present on L5, it is proposed to extend the lower range of this parameter to 1 MHz.
For the upper range of f_d, the main limiting factor is the signal generator's output filter bandwidth. For L5 signals, the output filter bandwidth is 24 MHz, instead of 20 MHz for L1 C/A signals. Therefore, higher frequency oscillations may be let out by the satellite payload, which leads to the proposition to extend the higher range of this parameter to 24 MHz.
For the parameter σ, lower values than 0.8 MNepers/s would result in unstable oscillation on the chips and are unlikely from a payload manufacturer point of view. Higher values than 8.8 MHz would not add any visible degradation. It is proposed to keep the same parameter range.

This proposition is summarized in Table 2. It is further confirmed when looking at the impact of the TM on the measurements using new modulations. Works like [6] or [7] show that the pseudo-range bias created by the proposed L5 threat model will have a worst case pseudo-range error of similar order of magnitude than the ICAO L1 C/A threat model, ie a few meters, thus confirming the need to monitor this kind of threat.

User design space and protected regions for L1 and L5

The term User Design space refers to the values of pre-correlation bandwidth and correlator spacing that a receiver uses for tracking a signal. Indeed, GNSS receivers have specific parameters depending on their manufacturer and targeted audience / cost / performances.

Table 2 – Proposed Threat Model parameters for L5

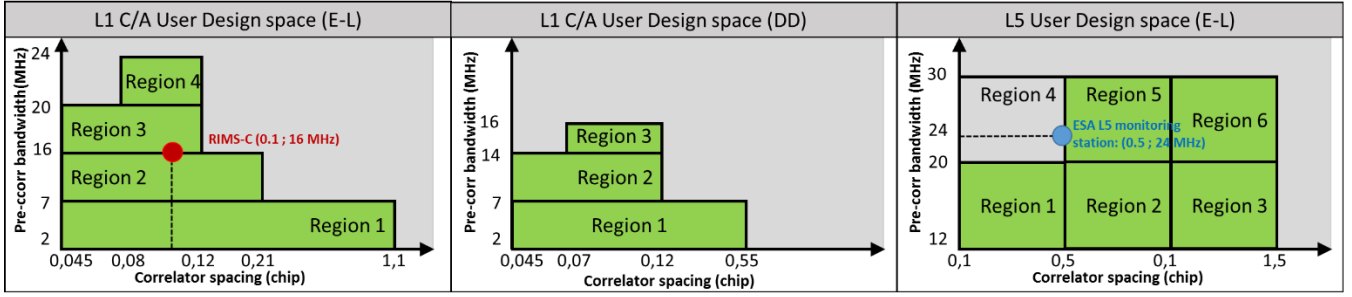|	Δ (chip)	σ (MNepers/s)	f_d (MHz)
TM A	[-0.6 ; 0.6]	-	-
TM B	-	[0.8 ; 8.8]	[1 ; 24]
TM C	[-0.6 ; 0.6]	[0.8 ; 8.8]	[1 ; 24]

**Figure 2 – User design space and protected regions (in green) for
(a) GPS L1 C/A Early Minus Late, (b) GPS L1 C/A Double Delta, (c) GPS L5 users**

The pre-correlation bandwidth corresponds to the bandwidth of the filter of the RF front-end. Low values of pre-correlation bandwidth results in the rounding of the correlation shape, thus decreasing the overall accuracy of the correlation peak tracking. It would also result in the filtering of some of the EWF.

The correlator spacing is a parameter of the delay lock loop, corresponding to the spacing between the early correlator and the late correlator. Lower correlator spacing, associated with large bandwidth, will usually permit to reach better tracking accuracy and multipath robustness [8]. The chip spacing also depends on the type of discriminator used. For L1 C/A signals, both Early-Minus-Late (E-L) and Double Delta (DD) discriminators are considered, while for L5, only E-L is considered.

These parameters are essential since they will affect the error induced on the pseudo-range measurement by EWF. In particular, for differential users, if the reference and the rover receivers have different user design characteristics, the pseudo-range bias created by the EWF will not be appropriately corrected through differential correction.

Consequently, [3] has defined some protected regions in the user design space, where the users are confirmed to be protected against EWF, either through detection and alert to the user, or by confirming that the EWF will not create an error superior to a required threshold after differential corrections.

For the moment, no protected region has been standardized for GPS L5 signal, so the suggested regions are only a proposition of the authors, based on the results presented in this paper.

The considered user design spaces and the associated protected regions are shown in Figure 2.

GENERAL DESCRIPTION OF SQM

EWFs create some distortion on the correlation function. The main family of EWF monitoring algorithm, named **Signal Quality Monitoring (SQM)** [3] is based on the observation of the correlation function of the received signal at different points. By choosing the right combination of correlators, it is possible to observe an anomaly in the symmetry or on the slope of the correlation function.

SQM is based on the observation of 2 kinds of metrics:
- ratio metrics, defined in Eq. 1,
- symmetry metrics, defined in Eq. 2.

$$R_m = \frac{I_E^m}{I_P}, \text{ or } R_m = \frac{I_L^m}{I_p} \qquad \text{Eq. 1}$$

$$\Delta_m = \frac{I_E^m - I_L^m}{2 I_P} \qquad \text{Eq. 2}$$

Where,
- I_E^m, I_L^m, I_P stands for the early, late and prompt correlator value on the in-phase signal component.
- m is the index corresponding to a particular correlator pair.

These metrics are corrected so that their mean value in absence of EWF is equal to 0. The correction comprises the possible biases due to the definition of the metric and the effects of the pre-correlation filter on the metrics.

In EGNOS and LAAS [9], a particular version of SQM algorithm – called SQM2b – is used. It relies on three distinct pairs of correlators: one pair for tracking and two pairs for SQM metrics computation. The final detection test is done by checking if any one of the metrics exceeds a threshold T.

$$\gamma = \max\left(\frac{R_1}{T(R_1)}, \frac{R_2}{T(R_2)}, \frac{\Delta_1}{T(\Delta_1)}, \frac{\Delta_2}{T(\Delta_2)}\right) \geq 1$$

The detection threshold is determined with regards to the distribution of the metrics, in order to comply with a false alarm probability. Therefore, there is a need to model the distribution of the metrics, through models or measurements.

ADAPTATION OF SQM TO GPS L5 SIGNAL AND CONSIDERATION OF MODERN GPS L1 C/A RECEIVERS

The same SQM principle has been adapted to the GPS L5 signal. The main difference will be the location of the correlator pairs, which will be farther away from the prompt correlator when expressed in fraction of L5 chips, due to the limited bandwidth of the L5 signal. Indeed the

L5 correlation peak is rounded due to this limited bandwidth, which makes the area around the correlation peak inadequate for the observation of distortions.

Also, the study of SQM using modern L1 C/A receivers is of current interest, to check if the legacy SQM2b design is still valid with current monitoring receivers.

The first considered receiver is a commercial receiver dedicated to monitoring stations (Novatel G-III). This receiver has only been used with the GPS L1 signal due to the unavailability of an L5-compatible antenna. This receiver provides 13 correlator outputs on L1 C/A signals. The other considered receiver is a software receiver operated by the European Space Agency (ESA). This receiver is able to track both GPS L1 C/A and GPS L5 signals. This receiver provides 61 correlator outputs on L1 C/A signals, and 23 correlator outputs on L5 signals.
The values of the receiver parameters used in this study are given in Table 3.

The parameters of the current monitoring stations for EGNOS, called RIMS-C, are recalled in the first column. Note that the main difference between the considered receivers and the current monitoring receivers is the larger pre-correlation bandwidth used in the RF front-end.

Description of measurement datasets

The new thresholds for L5 and modern L1 C/A receivers are determined through a process aiming at respecting the requirements for false alarm probability (P_{fa}) and missed detection probability (P_{md}), based on different measurement datasets.

The measurement datasets consist in correlator outputs collected with the considered receivers. They are in 2 forms:
- Real time series of correlator outputs from a Novatel G-III receiver,
- Statistical parameters (standard deviation) of each correlator outputs from Novatel G-III and ESA receivers. See Figure 3 for an illustration of such data for the ESA L1 dataset.

Four datasets are used in this study, shown in Table 4. They are representative of the receiving conditions of GNSS signals in monitoring stations. In particular, the data

coming from the ESA receiver is a concatenation of several data collection done at different sites, thus providing some kind of spatial diversity with regards to the constellation geometry.
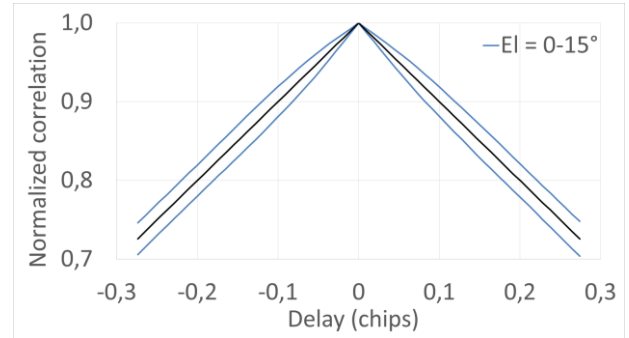

Figure 3 – Illustration of statistical data: 1-σ envelope of the correlator outputs for ESA receiver on L1

Determination of detection thresholds

The considered P_{fa} and P_{md} required as inputs for the threshold determination are deduced from the initial system requirements and the system implementation. The initial system requirements are:
- A false alarm probability $P_{fa}^0 = 1.5.10^{-7}$ per epoch, per satellite and per metric
- A missed detection probability $P_{md}^0 = 1.10^{-3}$ per satellite failure
- A Maximum Error Range Residuals (MERR) under 3.5m. The MERR is the maximum undetected error tolerable at the airborne receiver after differential corrections. Tolerable means that the error will not produce any hazardous misleading information. The chosen value corresponds to the maximum tolerable error for a GAD B system at 5° elevation [10].

The methodology to derive the P_{fa} and P_{md} required for the threshold determination at the monitoring station level depends on the system implementation, with parameters such as the number of monitoring stations, the number of monitoring receivers per monitoring stations, the voting algorithm, etc. Details on this implementation in the EGNOS system cannot be provided in this article. For this study, the considered P_{fa} is $3.162.10^{-4}$ and the considered P_{md} is $1.82.10^{-2}$.

Table 3 – Receiver assumptions for L1 and L5

	RIMS-C, L1	Novatel G-III, L1	ESA, L1	ESA, L5
Pre-correlation bandwidth (MHz)	16	24		
Pre-correlation filter type	6th order Butterworth			
Corr. spacing for tracking (chip)	0.10	0.10	0.365	0.5
Corr. spacing for monitoring (chip)	0.15, 0.20	0.15, 0.20	0.15, 0.2	1.28, 1.10

Table 4 – Multipath data sets characteristics

	Type of data	Siting	Frequency band	Receiver
Data set #1	Time series	Capgemini, Bayonne	L1	Novatel G-III
Data set #2	Statistical	Capgemini, Bayonne	L1	Novatel G-III
Data set #3	Statistical	Multiple sites	L1	ESA SW receiver
Data set #4	Statistical	Multiple sites	L5	ESA SW receiver

For statistical data sets, thresholds determination has been made following the steps detailed below:

1. Determination of the metrics distribution from the data sets by using the standard deviation of the metrics for low elevation (0 to 15°) and assuming that metrics have a Gaussian distribution. Metrics' standard deviations are assumed to follow the formulas given below:

$$\sigma_{R_m} = \sigma_{I_E^m} \text{ or } \sigma_{I_L^m}$$

$$\sigma_{\Delta_m} = 0.5 * \sqrt{\sigma_{I_E^m}^2 + \sigma_{I_L^m}^2}$$

Where $\sigma_{I_E^m}$ and $\sigma_{I_L^m}$ are the standard deviations of the early and late correlator outputs of the m-th correlator pair. This model of the correlator outputs assumes that the different correlators are uncorrelated and that the prompt does not bring any additional noise.

2. Definition of the range of thresholds to be tested: from 3 to 7 standard deviations in order to guarantee the required P_{fa} and to have the better P_{md},

3. Selection of all sets of thresholds that ensure the required P_{fa}: the P_{fa} is computed for each set of thresholds thanks to the probability density functions of the four metrics,

4. Identification of the EWF that generate a pseudo-range error above 3.5m on corrected users of the protected regions in the User Design space,

5. Determination of the metrics distribution for the retained EWF: EWF are assumed to only have the impact of shifting the metrics' mean without changing their standard deviation,

6. For each retained EWF parameter, the P_{md} is calculated from the probability density functions of the four metrics affected by the retained EWF. The worst P_{md} among these retained EWF for a given threshold set is stored. This step corresponds to the identification of the least detectable EWF by the considered set of thresholds.

7. Determination of the best P_{md}: Thresholds ensuring the lowest stored P_{md} are selected.

For real time data sets, thresholds determination has been made following the steps detailed below:

1. Determination of the metrics distribution from the time series of correlator outputs, for satellites between 0 and 15° elevations.

2. Definition of the range of thresholds to be tested: from 10 to 12 standard deviations in order to guarantee the required P_{fa} and to have the better P_{md}. See the discussion towards the end of the article, on the non-Gaussian behavior of the real datasets, leading to these higher thresholds.

3. Selection of all sets of thresholds that ensure the required P_{fa}: the P_{fa} has been computed for each set of thresholds by normalizing each metric of the data sets by its threshold and incrementing the number of false alarms whenever at least one normalized metric exceeds one. The P_{fa} is then the ratio between the number of false alarms and the total number of data,

1. P_{md} determination and thresholds selection is then made as in steps 4-7 of the previous description.

The methodology for computing the thresholds is summarized in Figure 4 for real measurements.
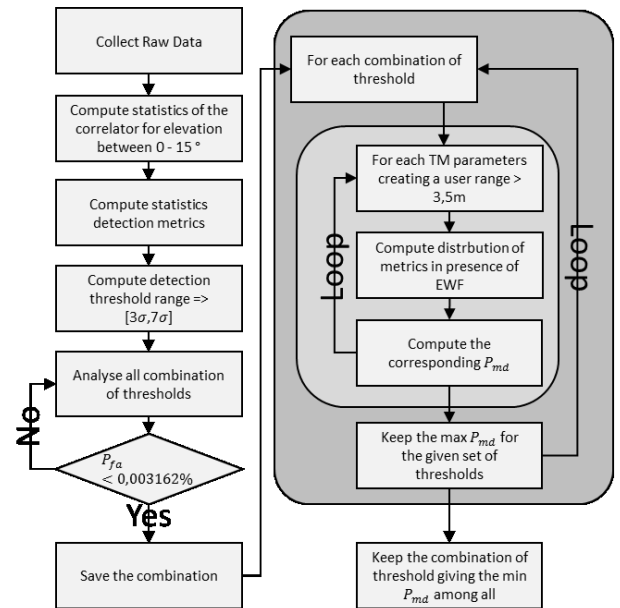

Figure 4 – Methodology for computing the detection threshold from raw data

SIMULATION OF SQM DETECTION PERFORMANCES

The presented methodology has been applied to the 4 datasets presented in Table 4. The SQM detection performances are assessed on 3 criteria:

#1 The P_{md} of the least detectable EWF creating a differential range error above 3.5 m,

#2 The percentage of undetected sets of TM parameters,

#3 The maximum range error for undetected EWF.

It is important to note that only criteria #1 is a requirement of ICAO. The other 2 criteria are presented for a qualitative assessment of the SQM algorithms.

Compliance of the P_{md} of the least detectable EWF with ICAO requirement

The EWF detection threshold methodology requires the computation of the first performance criterion. Indeed, the retained set of thresholds is chosen because it will give the best P_{md} for the least detectable EWF creating a differential range error above 3.5m for any users of the Protected Regions.

In order to further refine the analysis of the P_{md}, the analysis has been done for users of each Protected Regions of the User Design Space. It means that once the set of thresholds has been chosen thanks to the previous

methodology, the P_{md} of the least detectable EWF creating a differential range error above 3.5m, for a user of the designated Protected Region, is computed.

While the Protected Regions are defined by ICAO for L1, they are not defined for L5. Therefore, the L5 regions are chosen by dividing the User Design Space as shown in Figure 2.

The resulting region-specific P_{md} are given in Figure 5 and Figure 6. For L1 and L5, some regions highlighted in green are compliant with the required P_{md}.

For L1, a lot of regions are not compliant, which is quite surprising, since L1 SQM has been validated in prior works. Two causes could be at the origin of this results.

- The measurement datasets comprise large punctual errors, associated to very low elevation and to instants leading to loss-of-lock or convergence periods after reacquisition. Therefore, these large errors artificially increase the standard deviation of the dataset, and may also result in non-Gaussian distribution (especially in the tails of the distribution).
- The location of the monitoring correlator pairs was not optimized regarding the receiver configurations associated to the datasets.

For L5, the compliance is reached in most of the regions. This kind of results could be used to provide guidance for the definition of protected regions in the L5 User Design Space.
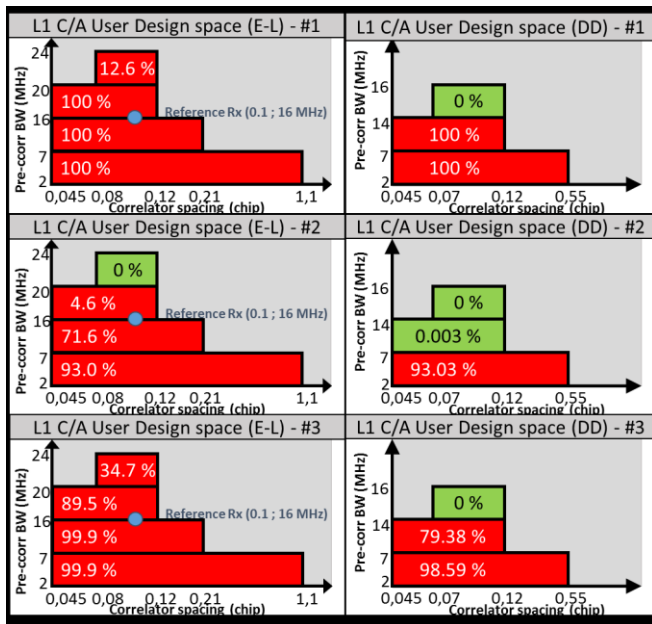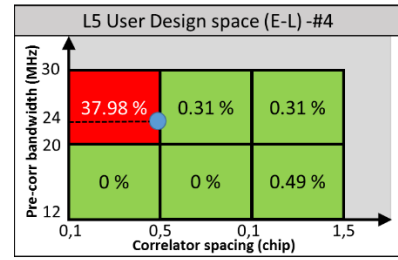

Figure 6 – P_{md} performances for the different Protected Regions of a L5 user, for dataset #4

SQM qualitative detection performances for different types of users

This section deals with the performance criteria #2 and #3. For these criteria, an EWF is considered as undetected if the *average* value of the metrics is below the detection threshold. There is no more consideration of the metrics standard deviation and missed detection probability. Figure 7 shows the exact methodology used for computing these criteria.

These criteria are obtained by testing each values of TM parameter range presented in
Table 1 and Table 2.
The increment on the parameter range is 0.01 chip for Δ, 1 MHz for f_d and 1 MNeper/s for σ for L1, and 0.1 chip for Δ, 1 MHz for f_d and 1 MNeper/s for σ for L5.
Also, a range of parameters of the user design space, consisting of a parameter couple {pre-correlation bandwidth, chip spacing} may be tested for the maximum range error determination, depending on the type of user considered, as explained below.
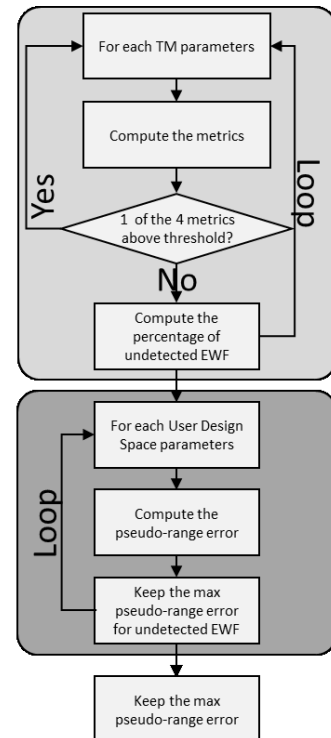

Figure 5 – P_{md} performances for the different Protected Regions of a L1 C/A user, for datasets #1-3

Figure 7 – Methodology for determining the qualitative SQM detection performance

Different types of users have been defined, depending on the use of SQM algorithms, the user design space and the use of differential corrections.

The 5 types of users are:

- **Independent user**. This user does not use SQM and its receiver parameters can take any values in the user design space. This is the worst-case user.
- **Monitoring station, without SQM**. This user is similar to the independent user, except that its receiver parameters are fixed to one set of parameter, detailed in Table 3.
- **Monitoring station, with SQM**. This user is similar to the previous user type, except that SQM is implemented. Therefore, the maximum range error will be chosen among the cases where an EWF is not detected, thus reducing it.
- **Protected user**. This user is protected by SQM, but its receiver parameters can take any values in protected regions of the user design space.
- **Corrected user**. This user is protected by SQM and its receiver parameters can take any values in the protected regions of the user design space. Additionally, differential corrections are used, so that the common range error between the reference station and the user is subtracted from the range error. This user is the best-case user.

In the case of the corrected user on L1, it should be mentioned that the monitoring receiver (RIMS-C for EGNOS) may have a different configuration than the reference receiver (RIMS-A), which computes the differential corrections. The reference receiver has the following parameters: $BW = 16$ MHz, $Cs = 0.1023$ chip. For L5, it has been assumed that the reference receiver has the same parameter as the monitoring receiver, ie $BW = 24$ MHz, $Cs = 0.5$ chip.

Figure 8 shows an example of detection performances of SQM on GPS L5 signals, using the L5 ESA receiver.
Figure 9 shows an example of contour plot used for the determination of the maximum range error for undetected EWF. This particular contour plot has been drafted for a corrected user using L5 signals.
Finally, Table 6 and Table 7, placed the end of the article, show the results for SQM detection performances for all types of users for all datasets.

Here are a few conclusions on this part of the study:

- Large differences between the different types of users can be observed, showing the importance of the implementation of SQM algorithms and the effectiveness of the limitation of the User Design Space to Protected Regions.
- For corrected users (which are the users targeted by a system such as SBAS), users using the L1 signal with modern receivers are found to be affected by large undetected differential pseudo-range error, above the required 3.5 m threshold. Also, the low number of detected EWF confirms that either the detection

threshold or the monitor design is not adapted to the monitoring function.

- For corrected users, users using L5 signals fulfill the requirement of maximum undetected differential pseudo-range error below 3.5 m.
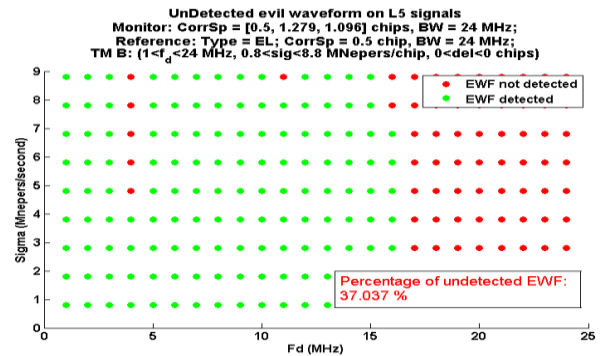

Figure 8 – Simulation of SQM detection performances on L5 for TM-B
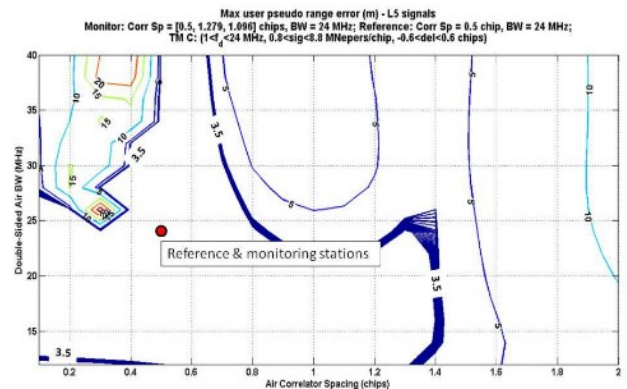

Figure 9 – Contour plot for determination of maximum pseudo-range error for a corrected user using L5 signals

DISCUSSION ON THE USE OF STATISTICAL DATA FOR THRESHOLD DETERMINATION

Before concluding this article, the authors would like to point out two interesting aspects encountered in this study. One particularity of this study has been to take into account 2 kinds of data for the threshold computation: statistical data (standard deviation of correlator outputs) and raw data (time series of correlator outputs recorded during 30 hours).

Datasets #1 and #2 were collected in order to study the possible limitations of considering statistical data. Indeed, the standard deviation of each correlator computed for dataset #2 is coming from the same time series used in dataset #1.

Gaussian approximation of the metrics distribution

The comparative analysis of the metrics distribution under the different assumptions shows that the distribution of the real correlator outputs is not Gaussian, especially towards the tails of the distribution, as shown in Figure 10.

This notably leads to high values of the metrics, especially at low elevation. This leads to the consideration of a much higher detection threshold for dataset #1, in order to be able to comply with a given P_{fa}, thus leading to worse missed detection performances.

This comparison shows that the use of statistical data lead to optimistic SQM performances, as can be observed when comparing datasets #1 and #2. Datasets #2 provides better performances in terms of P_{md} than dataset #1, while there are coming from exactly the same measurements.

One way to improve the situation, and make the metrics distribution more Gaussian-shaped, would be to exclude some outliers in the data collection, or to assess the distribution after an elevation mask.
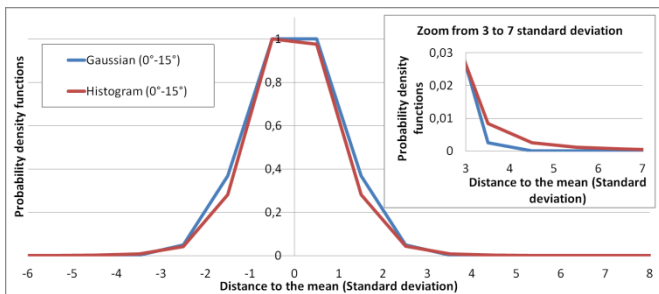

Figure 10 – Comparison of the distribution of real Δ_1 metrics (dataset #1) and the Gaussian assumption (dataset #2)

Correlation between the metrics

Another potentially abusive assumption of the statistical dataset was to consider the noise on different metrics as statistically independent, as no correlation coefficient was available.
However, in reality, the noise and multipath effects on the correlation function are correlated. Therefore, the metrics' behavior may not reflect reality when considering this uncorrelated correlators.

This is shown in Figure 11, where it can be observed that the two Δ metrics are correlated in dataset #1, contrary to the metrics generated from dataset #2.
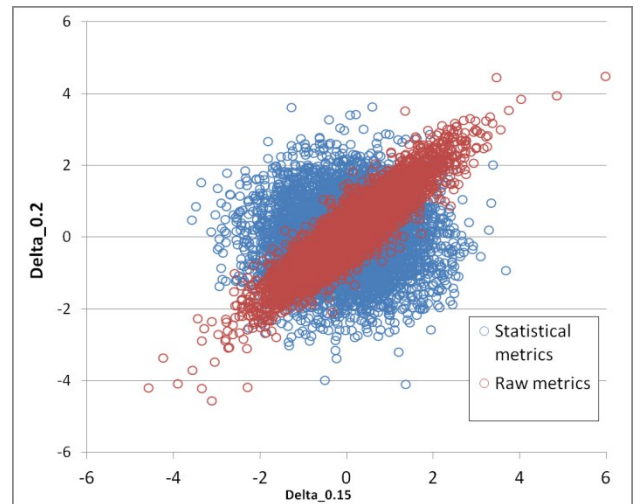

Figure 11 – Illustration of the correlation of metrics in dataset #1 (red) and dataset #2 (blue)

Similar correlation has been observed between the different metrics. The Pearson product moments correlation coefficient $\rho_{x,y}$ have been computed for couple of metrics in Table 5 and illustrated in Figure 12.

$$\rho_{x,y} = \frac{cov(X,Y)}{\sigma_x \sigma_y}$$

Table 5 – correlation coefficient between the different metrics in dataset #1

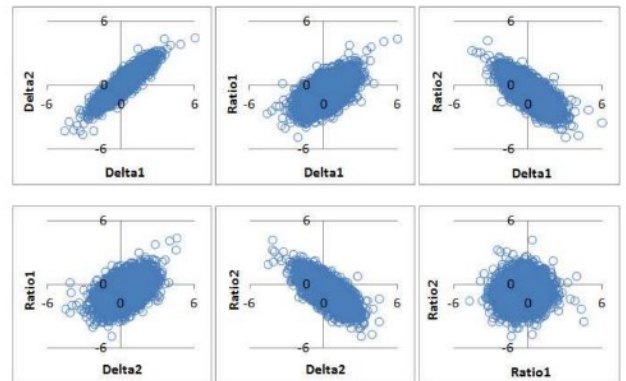|	Δ_1	Δ_2	R_1	R_2
Δ_1	1	0.91	0.54	-0.73
Δ_2	0.91	1	0.45	-0.71
R_1	0.54	0.45	1	0.17
R_2	-0.73	-0.71	0.17	1

Figure 12 – Illustration of the correlation between the different SQM metrics

When using a statistical dataset, the sets of detection thresholds are determined together so that the overall test (ie that at least one of the four metrics exceeds its threshold) provides the required P_{fa}, assuming independent Gaussian distribution for each metrics. However, taking into account a correlation between the metrics would yield different sets of thresholds.
On the other side, this correlation between metrics is taken into account when considering the real time series.

CONCLUSION AND FUTURE WORK

This paper has presented a methodology to compute the SQM monitoring detection thresholds based on different datasets.

The methodology has been applied to datasets corresponding to three L1 C/A data collection with modern receivers, and one L5 data collection.

Compliance with the required P_{md} for the least detectable EWF creating a differential range error above 3.5m, requested by ICAO has been assessed.

The SQM qualitative detection performances have been determined through the percentage of detected EWF. For undetected EWF, the maximum (differential) pseudo-range error is also provided. The SQM detection performances were computed for different types of users.

The study shows that the current implementation of SQM algorithms does not provide satisfactory performances on L1 C/A signals, with modern receivers, and with the detection threshold methodology. On the contrary, L5 signals can be adequately monitored with adapted SQM algorithms.

An other result is the dependency of the SQM detection performances to the region of the User Design space. Some regions are better protected than others, and would comply with the targeted requirement. This analysis by region can be useful to define the protected region for L5 users.

Finally, the use of statistical description of correlator outputs requires some particular attention. Notably, when analyzing true time series of correlator outputs, a non-Gaussian distribution of the metrics can be observed, together with a correlation between the different metrics. It is advised to either restrain the use of statistical description of correlator outputs, and to privilege real time series, or to complexify the modeling of the correlator outputs by introducing correlation between the metrics and a model of outliers. Also, the removal of some data on the real time series, for example, very low elevation data, or data corresponding to the convergence period of the tracking loops after a reacquisition may also be recommended.

Future work on this topic includes the adaptation of the SQM algorithm to modern L1 C/A receivers, by finding a new location of monitoring correlator pairs. With newer receiver, it is also possible to have more correlator pairs, thus opening the possibility to monitor distortions with more than 4 metrics and with more points of the correlation function. Finally, new combination of several metrics to comply with a global P_{fa} may be researched, taking into account the correlation between metrics and other voting scheme than a single threshold crossing.

ACKNOWLEDGMENTS

Table 6 - SQM detection performances results for L1 datasets

User type	Dataset	TM-A Percentage of detected EWF	TM-A PRE (m) E-L	TM-A PRE (m) DD	TM-B Percentage of detected EWF	TM-B PRE (m) E-L	TM-B PRE (m) DD	TM-C Percentage of detected EWF	TM-C PRE (m) E-L	TM-C PRE (m) DD
Corrected user	Novatel G-III (raw)	0	5.9	16.3	0	10	25.4	5.4	10.2	17.7
	Novatel G-III (stat)	38.5	1.4	2.9	27	7	5.1	5.4	6.3	7
	ESA (stat)	0	5.9	16.3	7.9	7	6,9	11.5	10.2	17.7

Table 7 - SQM detection performances results for ESA L5 (ESA statistical dataset)

User type	SQM	TM-A Percentage of detected EWF	TM-A PRE (m)	TM-B Percentage of detected EWF	TM-B PRE (m)	TM-C Percentage of detected EWF	TM-C PRE (m)
Independent user	No	NA	9.8	NA	69.5	NA	78.5
Monitoring station			7.8		67.1		76.1
Monitoring station	Yes	28.6	5.4	63	15.5	55.6	19.6
Protected user			6.5		15.8		19.9
Corrected user			1.0		2.4		2.5

REFERENCES

[1] Edgar C., Czopek F., Barker B., "A Co-operative Anomaly Resolution on PRN-19," Proceedings of the 12th International Technical Meeting of the Satellite Division of The Institute of Navigation (ION GPS 1999), Nashville, TN, September 1999, pp. 2269-2268.

[2] International Standards and Recommended Practices. Annex 10 to. ICAO. 6th Edition. July 2006.

[3] Phelts R. E. (2001). Multicorrelator techniques for robust mitigation of threats to GPS signal quality (Doctoral dissertation, Stanford University).

[4] Interface Specification IS-GPS-705C. Navstar GPS Space Segment/User Segment L5 Interfaces. Sep 2012.

[5] Wong, G., Phelts R.E., Walter T., Enge P., "Characterization of Signal Deformations for GPS and WAAS Satellites," Proceedings of the 23rd International Technical Meeting of The Satellite Division of the Institute of Navigation (ION GNSS 2010), Portland, OR, September 2010, pp. 3143-3151.

[6] Phelts E., Akos D., "Effects of Signal Deformations on Modernized GNSS Signals," Journal of Global Positioning Systems, Vol. 5, No. 1-2, 2006, 9 pp.

[7] Fontanella D., Paonni M., Eissfeller B., "A Novel Evil Waveforms Threat Model for New Generation GNSS signals: Theoretical Analysis and Performance," Satellite Navigation Technologies and European Workshop on GNSS Signals and Signal Processing (NAVITEC), 2010 5th ESA Workshop on , vol., no., pp.1,8, 8-10 Dec. 2010

[8] Van Dierendonck A. J., Fenton P., Ford T., "Theory and Performance of Narrow Correlator Spacing in a GPS Receiver", NAVIGATION, Journal of The Institute of Navigation, Vol. 39, No. 3, Fall 1992, pp. 265-284.

[9] Phelts R. E., Akos D. M., Enge P., "Robust Signal Quality Monitoring and Detection of Evil Waveforms," Proceedings of the 13th International Technical Meeting of the Satellite Division of The Institute of Navigation (ION GPS 2000), Salt Lake City, UT, September 2000, pp. 1180-1190.

[10] "Minimum Aviation System Performance Standards for Local Area Augmentation System (LAAS)," 2004.